Published for SISSA by Springer

Received: *October 10, 2022*
Accepted: *October 22, 2022*
Published: *November 2, 2022*

Bootstrapping conformal QED$_3$ and deconfined quantum critical point

Zhijin Li

Shing-Tung Yau Center and School of Phyiscs, Southeast University,
Nanjing 210096, China
Centro de Física do Porto, Departamento de Física e Astronomia,
Faculdade de Ciências da Universidade do Porto,
Rua do Campo Alegre 687, 4169–007 Porto, Portugal
Department of Physics, Yale University,
New Haven, CT 06511, U.S.A.

E-mail: zhijin_li@seu.edu.cn

Abstract: We bootstrap the deconfined quantum critical point (DQCP) and 3D Quantum Electrodynamics (QED$_3$) coupled to N_f flavors of two-component Dirac fermions. We show the lattice and perturbative results on the SO(5) symmetric DQCP are excluded by the bootstrap bounds with an assumption that the lowest singlet scalar is irrelevant. Remarkably, we discover a new family of kinks in the 3D SO(N) vector bootstrap bounds with $N \geqslant 6$. We demonstrate coincidences between SU(N_f) adjoint and SO(N_f^2-1) vector bootstrap bounds due to a novel algebraic relation between the crossing equations. By introducing gap assumptions breaking the SO(N_f^2-1) symmetry, the SU(N_f) adjoint bootstrap bounds with large N_f converge to the $1/N_f$ perturbative results of QED$_3$. Our results provide strong evidence that the SO(5) DQCP is not continuous and the critical flavor number of QED$_3$ is slightly above 2: $N_f^* \in (2,4)$. Bootstrap results near N_f^* are well consistent with the merger and annihilation mechanism for the loss of conformality in QED$_3$.

Keywords: Nonperturbative Effects, Scale and Conformal Symmetries, Global Symmetries

ArXiv ePrint: 1812.09281

https://doi.org/10.1007/JHEP11(2022)005

JHEP11(2022)005

Contents

1 Introduction

The 3D Quantum Electrodynamics (QED$_3$) has been extensively studied in the past 30 years. In the low energy limit the theory becomes strongly coupled and provides an interesting laboratory to study confinement and chiral symmetry breaking. The infrared (IR) phase of QED$_3$ is determined by the number of fermions charged under the U(1) gauge symmetry. The pure U(1) gauge theory ($N_f = 0$) confines [1, 2]. In the large N_f limit QED$_3$ can be solved using $1/N_f$ expansion which gives an interacting stable IR fixed point [3]. The IR phase of QED$_3$ is quite subtle with small N_f: the parity conserved mass of fermions could be generated dynamically and trigger spontaneously chiral symmetry breaking [4, 5].[1] There is a critical flavor number N_f^* which separates the conformal phase from chiral symmetry breaking phase. It is of critical importance to determine N_f^* for the applications of QED$_3$. For instance, $N_f = 4$ QED$_3$ has been applied to high-temperature cuprate superconductors [6, 7] and the order of phase transition is determined by N_f^*. Various approaches have been employed to estimate N_f^* without a conclusive answer [8–25].

The $N_f = 2$ QED$_3$ has been proposed to describe the deconfined quantum critical point (DQCP) [26]. A paradigmatic example of DQCP is the phase transition between Néel and Valence Bond Solid phases of quantum antiferromagnets on the 2D square lattice. In the

[1]The chiral invariant but parity violating fermion mass could be generated dynamically as well, however, it costs more energy comparing with the parity invariant one so is less favored [5].

continuum limit, this phase transition is described by the non-compact CP^1 (NCCP^1) model with $O(2)\times O(2)$ or SO(3) $\times$ U(1) symmetry, which are conjectured to be dual to the $N_f = 2$ QED$_3$ itself or coupled with a critical boson, i.e., the QED$_3$-GNY model. The two theories are further conjectured to be self-dual with $O(4)$/SO(5) symmetry enhancements and part of the 3D duality web [27–29], see [30] for a review. This scenario has been carefully studied using lattice simulations [31–36]. There is promising evidence for symmetry enhancement while it is not clear whether the phase transition is continuous or weakly first order.

Modern conformal bootstrap [37, 38] provides a powerful nonperturbative approach to study strongly coupled theories. Bootstrap studies on conformal QED$_3$ and DQCPs have been conducted in [39–44] which provide strict necessary conditions for the CFT data, though no clear evidence showing the bounds are saturated by conformal QED$_3$. In this work, we extend bootstrap studies of the SO(5) symmetric DQCP and conformal QED$_3$. Our results shed new light for several widely interested problems of these strongly coupled theories.

2 Bootstrap bounds on SO(5) DQCP

The SO(5) symmetric DQCP has been suggested to be described by either NCCP^1 model or $N_f = 2$ QED$_3$-GNY model [29]. In NCCP^1 model, the SO(5) vector multiplet contains the half-charged monopole and Néel order parameter; while in $N_f = 2$ QED$_3$-GNY model, it consists of a critical boson and the half-charged monopoles. Besides, the leading SO(5) traceless symmetric (T) scalar is constructed by the charge 1 monopoles and fermion bilinears in $N_f = 2$ QED$_3$-GNY model or quadrilinear of the matter fields in NCCP^1 model. Above recipes of SO(5) representations are helpful to test the emergent SO(5) symmetry and dualities using lattice simulations [31, 32, 45–47] or perturbative approaches [17, 48–50]. The results provide promising evidence for the emergent SO(5) symmetry and dualities. Nevertheless, the lattice simulations in [31] observed drifting in the critical indices, indicating the IR phase is subtle.

In figures 1–2 we show bootstrap bounds with $\Lambda = 31$,[2] on scaling dimensions of the lowest singlet (Δ_{Sig}) and traceless symmetric scalar (Δ_T) in any unitary 3D SO(5) symmetric CFTs. The bounds are smooth in most of the regions except sharp kinks in the left-bottom corner corresponding to the critical $O(5)$ vector model [52]. The lowest SO(5) singlet scalar has to be irrelevant to realize the SO(5) DQCP in lattice simulations without fine-tuning. Otherwise a relevant singlet scalar can introduce a non-negligible perturbation to the theory which drives the RG flows away from the fixed point. The presumed SO(5) symmetric DQCP will be unstable under this perturbation and cannot be directly reached in the long distance limit. The condition $\Delta_{\text{Sig}} > 3$ leads to a lower cut on the SO(5) vector scaling dimension $\Delta_\phi > 0.79$. A slightly weaker lower cut on Δ_ϕ has been obtained independently in [42], see [38] for discussions. In figure 2 we compared our bootstrap bounds with lattice simulations [31, 32, 45–47] and perturbative results [17, 48–50] on the SO(5) DQCP, which are summarized in table 1.[3] Most of the estimates on Δ_ϕ locate in the range

[2] In bootstrap computations, Λ is the order of the highest derivative in the linear functional, which determines the numerical precision [51]. Unless specified explicitly, we will use $\Lambda = 31$ throughout this paper.

[3] Note the critical indices from the lattice simulation [31] can drift to smaller values, e.g. $\Delta_T \simeq 0.895^{85}$ with larger lattice sizes. The two sets of values in [50] are obtained from Padé and Borel-Padé approximations.

JHEP11(2022)005

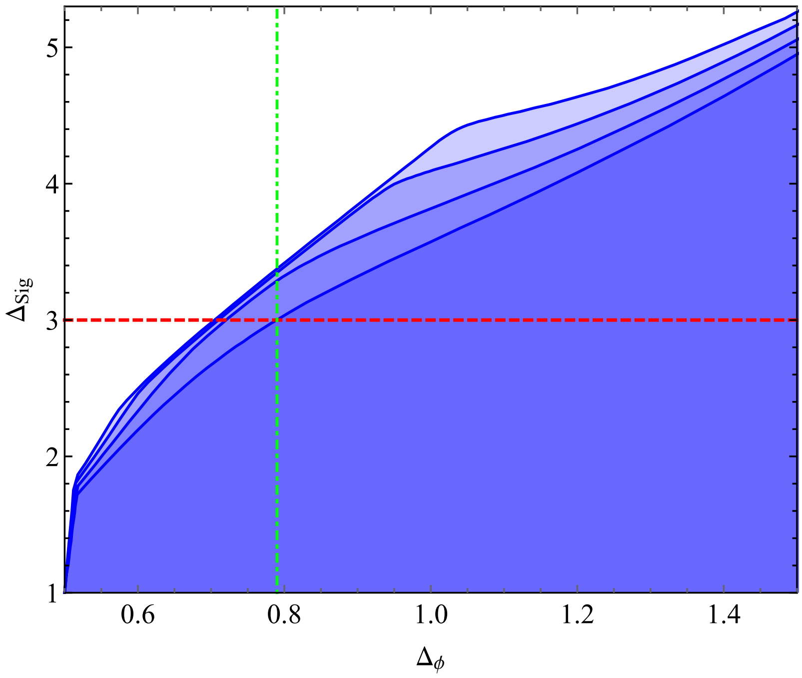

Figure 1. Upper bounds ($\Lambda = 31$) on the scaling dimensions of the SO(N) singlet scalars. $N = 5, 6, 7, 8$ from bottom to top. The dot-dashed green line gives a left cut for the SO(5) singlet bound with a gap assumption $\Delta_{\text{Sig}} > 3$.

Refs.	[45]	[46]	[47]	[31]	[48]	[49]	[50]
Δ_ϕ	0.630^{15}	0.675^{15}	0.64^{4}	0.625^{15}	0.63	0.65	0.59/0.65
Δ_T	1.716^{50}	1.52^{9}	1.11^{20}	1.39^{3}	1.50	1.58	1.42/1.51

Table 1. CFT data of SO(5) DQCP (=est.$^{\text{err.}}$) estimated from lattice simulations or $1/N_f$ expansions.

(0.6, 0.7), notably smaller than the lower cut $\Delta_\phi > 0.79$. Therefore if the SO(5) DQCP is described by a unitary CFT with an SO(5) vector given in table 1, there has to be a relevant singlet scalar, which necessarily affects the IR phase in the lattice simulations. The conclusion is that the phase transitions observed in above lattice simulations cannot be both SO(5) symmetric and continuous.

However, bootstrap bounds in figures 1 and 2 do not exclude possible SO(5) symmetric CFTs with $\Delta_\phi \in (0.6, 0.7)$ and a relevant singlet scalar. This scenario gets more intriguing considering that in figure 2, part of the lattice and $1/N_f$ results locate near the upper bound on Δ_T without the gap assumption $\Delta_{\text{Sig}} > 3$. Nevertheless, a substantial challenge to realize such a presumed fixed point in lattice simulations is the fine tuning of the coefficient of the relevant SO(5) singlet operator. It would be interesting to know whether the data near SO(5) vector bootstrap bounds corresponds to a truly unitary CFT.

JHEP11(2022)005

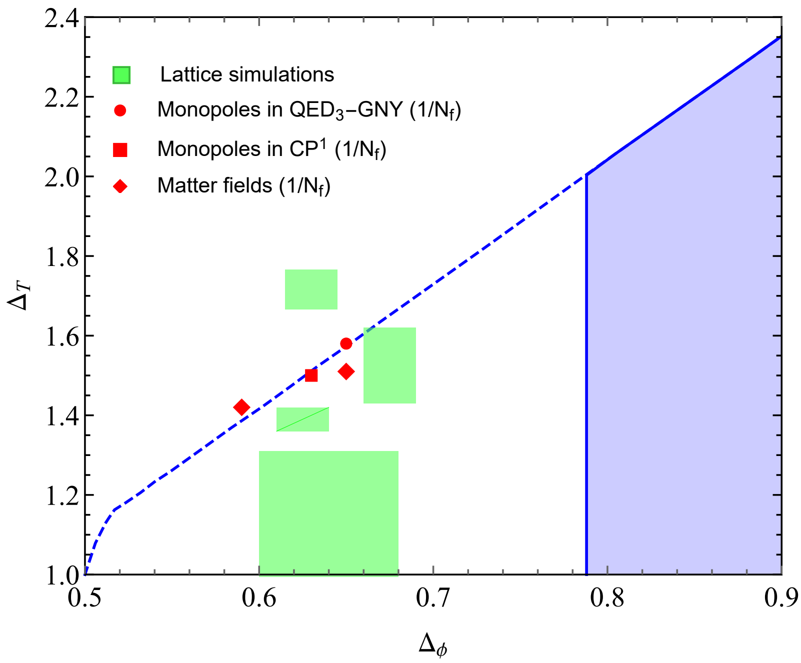

Figure 2. Dashed blue line: upper bound on the scaling dimension Δ_T. Blue shadowed region: bootstrap allowed region of (Δ_ϕ, Δ_T) with a gap assumption $\Delta_{\rm Sig} > 3$.

A remarkable observation in figure 1 is that the SO(N) singlet bounds show prominent kinks with irrelevant singlet scalars for $N \geqslant 7$![4] The kink becomes mild at $N = 6$ and disappears at $N = 5$, while the widely studied SO(5) DQCP is just below the conformal window of this new family of kinks! Moreover, the kinks disappear accompanied by the lowest singlet scalar crossing the marginality condition $\Delta_{\rm Sig} = 3$. This is particularly interesting to study the loss of conformality [8, 10, 11, 53–55] and we will discuss its possible interpretation later.

3 New family of kinks and QED$_3$

In the large N limit, the new family of kinks shown in figure 3 approach the scaling dimension of free fermion bilinears $\Delta_\phi = 2$ from below. If the kinks at finite N correspond to certain full-fledged CFTs, the underlying theories are expected to be fermionic theories equipped with gauge interactions. Otherwise, in the non-gauged fermionic theories like Gross-Neveu-Yukawa model, the fermion bilinears receive positive anomalous dimensions and approach $\Delta_\phi = 2$ from above [50, 56], which are opposite to the bootstrap results. It is tempting to conjecture they are given by the DQCPs with higher symmetries, e.g. $N_f = 4$ QED$_3$. More specifically, with large N the kinks show interesting fine structures in which there seem to be two nearby kinks in the bounds on SO(N) singlet $\Delta_{\rm\ Sig}$, and the

[4] Actually there are extra kinks in the $O(N)$ singlet bootstrap bounds for $N = 7, 8$, which have scaling dimensions $\Delta_\phi \sim 0.6, \Delta_S \sim 2.5$. It would be interesting to understand the underlying theories of these kinks.

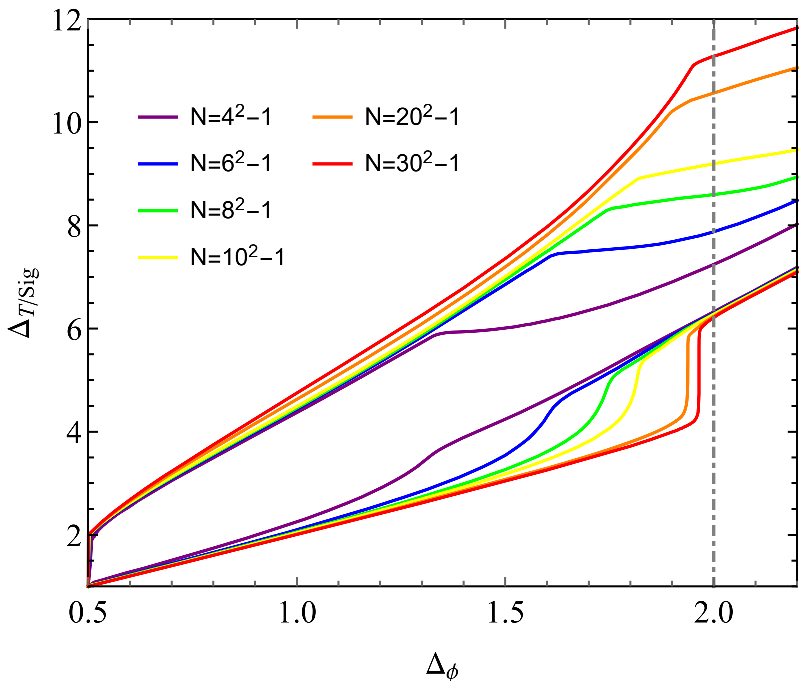

Figure 3. Bounds on Δ_{Sig} (upper set) and Δ_T (lower set) from SO(N) vector bootstrap.

Δ_ϕ of the two nearby kinks respectively locate in the bottom and top of the jumps in the bounds on the SO(N) traceless symmetric scalar Δ_T, see appendix B for examples and more discussions.[5] A challenge of this conjecture is that for large flavor QED$_3$, the theory does not have an SO(N) symmetry enhancement in the IR and the fermion bilinears transform as an SU(N_f) adjoint instead of SO(N) vector. This puzzle can be resolved by a novel SO(N_f^2-1) symmetric positive structure in the SU(N_f) adjoint crossing equations [57, 58].

3.1 A novel algebraic relation in the crossing equations

We bootstrap the SU(N_f) ($N_f \geqslant 4$) adjoint fermion bilinear $\mathcal{O}_{\mathrm{ad}}$ in QED$_3$. Its four-point crossing equations are given by the matrix [59, 60]

$$\begin{aligned}\mathcal{M}_{\mathrm{ad}} &\equiv \left(\vec{V}^+_{\mathbf{1}}, \vec{V}^+_{\mathrm{Ad}}, \vec{V}^-_{\mathrm{Ad}}, \vec{V}^-_{T\bar{A}}, \vec{V}^+_{A\bar{A}}, \vec{V}^+_{T\bar{T}}\right) \qquad (3.1)\\ &= \begin{pmatrix} 0 & 0 & 0 & -F & F & F \\ 0 & \frac{2F}{N_f} & 0 & 0 & -\frac{F}{N_f-2} & \frac{F}{N_f+2} \\ 0 & -F & -F & \frac{F}{N_f} & \frac{F}{N_f-2} & \frac{F}{N_f+2} \\ F & -\frac{16F}{N_f} & 0 & 0 & \frac{2N_f^2F}{(N_f-1)(N_f-2)} & \frac{2N_f^2F}{(N_f+1)(N_f+2)} \\ H & -\frac{4H}{N_f} & 0 & -H & -\frac{N_f(N_f-3)H}{(N_f-1)(N_f-2)} & -\frac{N_f(N_f+3)H}{(N_f+1)(N_f+2)} \\ 0 & H & -H & \frac{H}{N_f} & \frac{(N_f-3)H}{N_f-2} & -\frac{(N_f+3)H}{N_f+2} \end{pmatrix},\end{aligned}$$

[5]We will show that the first one of the two nearby kinks in the $O(N_f^2-1)$ vector bootstrap bound has Δ_ϕ close to the SU(N_f) adjoint fermion bilinear scaling dimension in QED$_3$. This kink has Δ_T near the bottom of the jump in the bound on Δ_T and it will be the main focus of this work. It will also be interesting to study the underlying theories of the another adjacent kink, which may relate to other gauge theories like QED$_3$-GN model with more subtleties to clarify.

where $F/H = v^{\Delta_{\mathcal{O}_{\rm ad}}} g_{\Delta,\ell}(u,v) \mp u^{\Delta_{\mathcal{O}_{\rm ad}}} g_{\Delta,\ell}(v,u)$ and $g_{\Delta,\ell}$ is the conformal block function [61, 62]. The vector $\vec{V}_\pi^{\pm}$ denotes contributions of operators in the π representation of $\mathrm{SU}(N_f)$ with even/odd spins. Surprisingly, $\mathcal{M}_{\rm ad}$ is related to the $\mathrm{SO}(N)$ vector crossing equations

$$\mathcal{M}_{\mathrm{SO}(N)} \equiv \left(\vec{V}^{+}_{\rm Sig}, \vec{V}^{+}_{T}, \vec{V}^{-}_{A}\right) = \begin{pmatrix} 0 & F & -F \\ F & \left(1-\frac{2}{N}\right)F & F \\ H & -\left(1+\frac{2}{N}\right)H & -H \end{pmatrix} \tag{3.2}$$

through a linear transformation [57, 58]

$$\mathscr{T}_{\rm ad} = \begin{pmatrix} 1 & \frac{2\left(N_f^4-2N_f^2+2\right)}{N_f^4-N_f^2-2} & \frac{2N_f}{N_f^2-2} & 0 & 0 & 0 \\ -1 & \frac{-8N_f^4+16N_f^2+4}{-N_f^4+N_f^2+2} & -\frac{2N_f}{N_f^2-2} & 1 & 0 & 0 \\ 0 & 0 & 0 & 0 & 1 & \frac{2N_f}{N_f^2-2} \end{pmatrix}, \tag{3.3}$$

which maps $\mathcal{M}_{\rm ad}$ to $\mathcal{M}_{\mathrm{SO}(N)}$ with $N = N_f^2-1$:

$$\mathscr{T}_{\rm ad}\cdot\mathcal{M}_{\rm ad} = \left(\vec{V}^{+}_{\rm Sig}, x_1\vec{V}^{+}_{T}, x_2\vec{V}^{-}_{A}, x_3\vec{V}^{-}_{A}, x_4\vec{V}^{+}_{T}, x_5\vec{V}^{+}_{T}\right), \tag{3.4}$$

associated with positive x_i and the branching rules

$$\begin{aligned} \mathrm{SO}(N_f^2-1) & \qquad\qquad \mathrm{SU}(N_f) \\ \mathrm{Sig} \quad &\longleftrightarrow \quad \mathbf{1}\,, && (3.5)\\ T \quad &\longleftrightarrow \quad \mathrm{Ad}^+ \oplus A\bar{A} \oplus T\bar{T}\,, && (3.6)\\ A \quad &\longleftrightarrow \quad \mathrm{Ad}^- \oplus T\bar{A}\,. && (3.7) \end{aligned}$$

The algebraic relation (3.4), when combined with the bootstrap algorithm, leads to the $\mathrm{SU}(N_f)$ adjoint and $\mathrm{SO}(N_f^2-1)$ vector bootstrap bound coincidences [58]. It also allows to construct an $\mathrm{SO}(N_f^2-1)$ symmetric four-point correlator deformed from the four-point correlator of $\mathcal{O}_{\rm ad}$, which satisfies the $\mathrm{SO}(N)$ vector crossing equations [58]. Now the question is if the new kinks are related to deformations of conformal QED$_3$ caused by the algebraic relation (3.4)? The solution to this problem requires precise CFT data and knowledge of the four-point correlator of $\mathcal{O}_{\rm ad}$, which are beyond our current scope. In this work, we verify the conjectured relation by disentangling the QED$_3$ bootstrap results from the algebraic relation (3.4): *if we break the* $\mathrm{SO}(N_f^2-1)$ *symmetry in the* $\mathrm{SU}(N_f)$ *adjoint bootstrap setup, will the bootstrap bounds converge to conformal QED$_3$?* The answer could tell us that besides the algebraic relation (3.4), is it conformal QED$_3$ or other ingredient involved in the bootstrap bounds.

3.2 SU(N_f) adjoint fermion bilinear bootstrap and QED$_3$ spectrum

The QED$_3$ spectrum breaks the $\mathrm{SO}(N_f^2-1)$ symmetry (3.5)–(3.7) from two aspects. Firstly, in (3.7) the $\mathrm{SO}(N_f^2-1)$ symmetry conserved current is decomposed into conserved currents

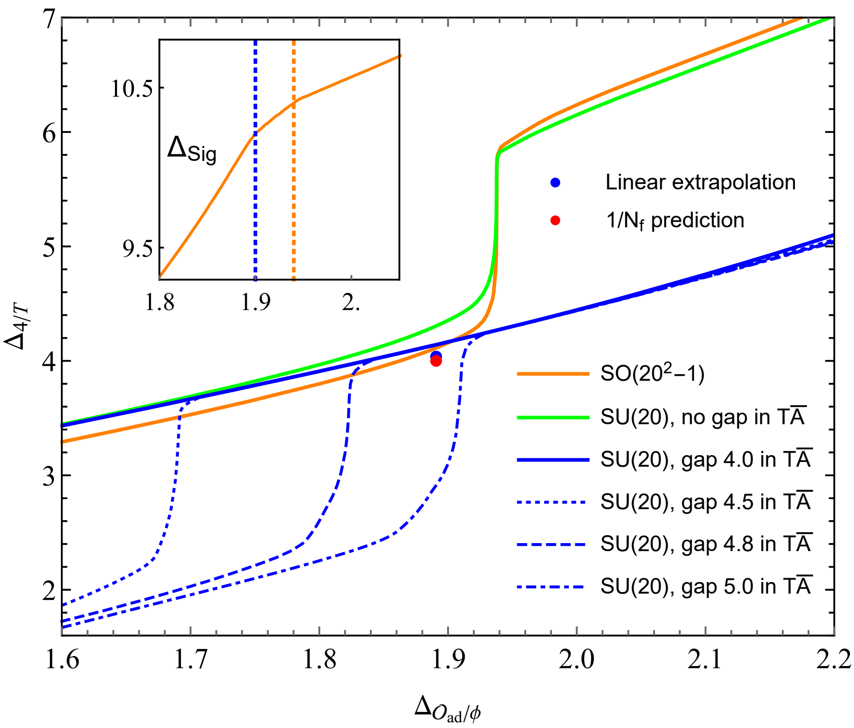

Figure 4. Bounds on Δ_4 and Δ_T from SU(20) adjoint and SO(399) vector bootstrap. In the left-top window, the orange line gives the singlet upper bound obtained from SO(399) vector bootstrap with two kinks near $\Delta_\phi = 1.90$ and 1.94.

in both Ad$^-$ and $T\bar{A}$ sectors, while in QED$_3$ the leading spin 1 operator in $T\bar{A}$ sector has scaling dimension $5 \pm O(1/N_f)$. Secondly, in the three SU(N_f) sectors branched from the SO(N_f^2-1) T sector (3.6), the leading scalars in QED$_3$ are the four-fermion operators, whose scaling dimensions violate the SO(N_f^2-1) symmetry at the subleading order [63, 64]:

$$(\Delta_{\rm Ad}, \Delta_{A\bar{A}}, \Delta_{T\bar{T}}) \simeq \left(4 - \frac{185}{3\pi^2 N_f}, 4 - \frac{64}{\pi^2 N_f}, 4 + \frac{64}{3\pi^2 N_f}\right). \tag{3.8}$$

We introduce gap assumptions inspired by above QED$_3$ spectrum in our bootstrap setup. Specifically, we require the lowest scalars in (3.6) satisfy:

$$\Delta \geqslant \left(\Delta_4 - \frac{185}{3\pi^2 N_f}, \Delta_4 - \frac{64}{\pi^2 N_f}, \Delta_4 + \frac{64}{3\pi^2 N_f}\right) \tag{3.9}$$

and bootstrap the upper bound on Δ_4. In the physical spectrum of QED$_3$ with large N_f, we have $\Delta_4 \simeq 4$. We will introduce different gaps Δ_1^* in the $T\bar{A}$ sector.

In figure 4 we show the bootstrap results for $N_f = 20$ QED$_3$, for which the $1/N_f$ expansions at subleading order are expected to be close to the physical spectrum. Note

N_f	10	20	30	50	100	150	200
Δ_4	4.083	4.038	4.024	4.017	4.005	4.004	4.001

Table 2. Linear extrapolations of the upper bounds on Δ_4 ($\simeq 4$ in QED$_3$ with large N_f) with $\Delta_{\mathcal{O}_{\rm ad}}$ fixed at the $1/N_f$ results. The upper bounds are not sensitive to the gap Δ_1^* and we fix it at $\Delta_1^* = 4$ in the computations.

before the jump the bound on Δ_4 has been shifted slightly from the SO(20^2-1) vector bootstrap bound (orange line) due to the SO(20^2-1) symmetry breaking gaps in (3.9), in contrast, such a shift disappears on the top of the jump and changes the direction after the jump. Interestingly, by introducing gaps $\Delta_1^* = 3.5, 4.0, \text{or } 4.5$ in the $T\bar{A}_{\ell=1}$ sector, the upper bounds on Δ_4 are almost the same, indicating the upper bound on Δ_4 is not sensitive to the specific value of gap Δ_1^*! Moreover, the gaps $\Delta_1^* = 4.5, 4.8, 5.0$ generate sharp jumps in the bounds on Δ_4! With a gap $\Delta_1^* = 5.0$ the large N_f predictions on QED$_3$ (red dot) are excluded while the gap $\Delta_1^* = 4.8$ generates a jump near the physical value $\Delta_4 = 4$. Coefficient of the $1/N_f$ term in $\Delta_1^* = 5 \pm O(1/N_f)$ is not known yet but our results suggest the subleading order correction should be negative! Using linear extrapolation of the upper bounds on Δ_4 with a gap $\Delta_1^* = 4$, it gives an optimal upper bound $\Delta_4 \simeq 4.038$ near $\Delta_{\mathcal{O}_{\rm ad}} \simeq 1.891$, remarkably close to the physical value $\Delta_4 = 4$! The small discrepancy could be explained by higher order corrections to the CFT data in (3.8).[6] More discussions on the bootstrap bounds are provided in appendix C.

In table 2 we show more comparisons between perturbative results and linear extrapolations of bounds on Δ_4.[7] Agreements between the two methods get more impressive with increasing N_f.

3.3 Lower bounds on c_J and c_T in SU(N_f) adjoint fermion bilinear bootstrap

The results in figure 4 suggest that the upper bound (blue line) on Δ_4 with gap assumptions breaking SO(20^2-1) symmetry converges to the $1/N_f$ perturbative results of $N_f = 20$ QED$_3$ in the large Λ limit. This provides promising evidence for that conformal QED$_3$ may provide a nearly extremal solution to the bootstrap bound with non-SO(20^2-1) symmetric gap assumptions, up to uncertainties from linear extrapolations. A widely concerned question in the fermion bilinear bootstrap is that the bootstrap implementations cannot distinguish theories with different gauge groups, e.g., QED$_3$ and QCD$_3$. For instance, the SU(N_f) adjoint fermion bilinears $\mathcal{O}_{\rm ad}$ appear both in QED$_3$ and QCD$_3$, and their scaling dimensions are the same at leading order with possibly different higher order corrections. In general the low lying gauge invariant operators constructed from matter fields are similar in these theories and it may be hard to distinguish QED$_3$ from Yang-Mill gauge theories with the same flavor symmetry.

[6]The subleading order corrections in (3.8) are at the order $O(10^{-1})$. One may expect the next-to-subleading order corrections at the order $O(10^{-2})$, comparable to the discrepancy. Note the results may also be affected by the systematical errors from linear extrapolation.

[7]Bootstrap results with $\Lambda = 19, 21, \ldots, 35$ used in the linear extrapolations are provided in an attached *Mathematica* file. We used binary search to compute upper bounds on Δ_4 with numerical precision 10^{-5}.

JHEP11(2022)005

A significant difference between QED$_3$ and QCD$_3$ appears in the central charges. In QCD$_3$, the fermions and gauge fields also carry color indices. These Yang-Mills theories contain larger degree of freedoms than the Abelian gauge theories. Such difference can be reflected in the central charges, which measure the degree of freedoms of the theories. In this subsection, we will study bootstrap bounds on the SU(20) conserved current central charge c_J and stress tensor central charge c_T with Δ_4 fixed near its upper bounds in figure 4. The bootstrap bounds on central charges can provide substantial information on whether the bootstrap bounds are related to the QED$_3$ or QCD$_3$.

The central charges c_J and c_T in QED$_3$ have been computed using $1/N_f$ perturbative method to subleading order [11]

$$c_J = c_{J0}\left(1+\frac{0.1429}{N_f}+O\left(\frac{1}{N_f^2}\right)\right), \tag{3.10}$$

$$c_T = c_{T0}\left(1+\frac{0.7193}{N_f}+O\left(\frac{1}{N_f^2}\right)\right), \tag{3.11}$$

where c_{J0} and c_{T0} are the central charges from N_f flavors of two-component free fermions. In contrast, the central charges in QCD$_3$ with an SU(N_c) gauge symmetry are given by [11]

$$c_J = N_c c_{J0}\left(1+\frac{0.1429}{N_f}\frac{N_c^2-1}{N_c}+O\left(\frac{1}{N_f^2}\right)\right), \tag{3.12}$$

$$c_T = N_c c_{T0}\left(1+\frac{0.7193}{N_f}\frac{N_c^2-1}{N_c}+O\left(\frac{1}{N_f^2}\right)\right), \tag{3.13}$$

which are nearly N_c times larger than those in QED$_3$. Therefore the central charges c_J and c_T can be employed to provide a quantitative check for the Abelian gauge theories. We will compare the above perturbative results on c_J and c_T central charges with the bootstrap bounds.

In figure 5 we show lower bounds on c_J and c_T with Δ_4 fixed near its upper bounds (blue and green lines in figure 4). On the bound of c_J without a gap in the $T\bar{A}$ sector, there is a sharp jump near $\Delta_{\mathcal{O}_{\rm ad}} = 1.94$, corresponding to the jump in the bound on Δ_4, given by the green line in figure 4. In this work, we will be particularly interested in the bounds near the physical spectrum of QED$_3$ (3.8): $\Delta_4 \simeq 4$, which intercepts the Δ_4 upper bound (blue line) in figure 4 at $\Delta_{\mathcal{O}_{\rm ad}} \sim 1.836$. The scaling dimension $\Delta_{\mathcal{O}_{\rm ad}} \sim 1.836$ with $\Delta_4 = 4$ is obtained at $\Lambda = 31$, which is lower than the $1/N_f$ perturbative result $\Delta_{\mathcal{O}_{\rm ad}} \sim 1.891$. Using linear extrapolations, the two estimates become reasonably close with each other in the large Λ limit, as shown in figure 4 and table 2. Remarkably, near $\Delta_4 = 4$, lower bounds on c_J and c_T given by the red dots in figure 5 are quite close to the large N_f perturbative results (3.10). Note that both c_J and c_T change drastically with $\Delta_{\mathcal{O}_{\rm ad}}$, it is highly non-trivial that bounds on c_J and c_T get close to their physical value just near $\Delta_4 = 4$. As we have discussed before, c_J and c_T in Yang-Mills gauge theories, like QCD$_3$ have c_J and c_T about N_c times larger than the bounds in figure 5. Therefore the underlying theory near the bounds on c_J and c_T at $\Delta_4 = 4$ should be QED$_3$ or analogous 3D Abelian gauge theories instead of Yang-Mills gauge theories.

Another interesting question is why do the bootstrap results relate to QED$_3$ instead of QED$_3$ with Chern-Simons coupling? Both of the two theories are Abelian gauge theories

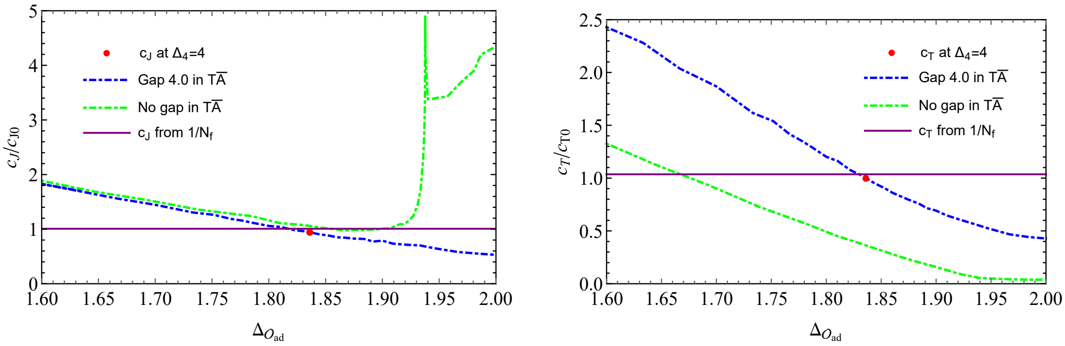

Figure 5. Lower bounds on central charges c_J (left panel) and c_T (right panel) near the upper bounds on Δ_4 with/without a gap $\Delta_1^* = 4$ in figure 4. The central charges are given with the normalization in which $c_J = c_T = 1$ for $N_f = 20$ two-component free fermions. The sharp pike in the c_J lower bound without $T\bar{A}$ gap (green line in the left panel) can be affected by our sample points near the jump in Δ_4 bound in figure 4. Clearly there is a jump in c_J bound near $\Delta_{\mathcal{O}_{\rm ad}} = 1.94$, but the shape of the bound right to the jump may change notably if our sample points get more close to the boundary.

and are expected to have close central charges. As a result one cannot distinguish them using central charges. This question can be well answered due to two reasons. First, with Chern-Simons coupling the theory breaks Parity symmetry, therefore the lowest scalar in the Ad$^+$ sector is the SU(N_f) adjoint fermion bilinear operator, which has scaling dimension $\Delta_{\mathcal{O}_{\rm ad}}$, significantly lower than the lowest parity even SU(N_f) adjoint scalar, therefore the QED$_3$-Chern-Simons theory locates in the region well below the bootstrap bounds. Second, for the N_f flavor QED$_3$ with a Chern-Simons coupling at level k, the SU(N_f) adjoint fermion bilinear scalar has modified scaling dimension [65]:

$$\Delta_{\mathcal{O}_{\rm ad}} = 2 - \frac{64}{3\pi^2(1+\lambda^2)N_f}, \tag{3.14}$$

where $\lambda = 8k/\pi N_f$. The scaling dimension of the SU(N_f) adjoint fermion bilinear scalar increases with larger k. Therefore the QED$_3$-Chern-Simons theory with $k > 0$ locate in the region right to the QED$_3$ theory with $k = 0$.

3.4 Comments on the fermion bilinear bootstrap results

The results provide strong evidence for the question we want to address: *the* SU(N_f) *adjoint bootstrap bounds, after resolving the* SO($N_f^2 - 1$) *symmetry enhancement, are close to be saturated by conformal QED*$_3$*!* This supports the conjectured relation between the new kinks and conformal QED$_3$, though details in this relation are not yet clarified.

Let us go back to the observation in figure 1 that the kinks disappear with the lowest singlet scalar crossing marginality condition. According to the proposed relation between the new kinks and conformal QED$_3$, disappearance of the kinks relates to loss of conformality in QED$_3$, indicating a critical flavor number slightly above 2: $N_f^* \in (2, 4)$. In consequence, the DQCPs related to $N_f = 2$ QED$_3$ or QED$_3$-GNY model may violate unitarity by a small complex factor, which explains the quasi-conformal behavior observed in lattice simulations [55, 66]. The marginally irrelevant scalar near N_f^* can be nicely interpreted by the merger and annihilation mechanism for the loss of conformality in QED$_3$ [54, 55]. In this scenario, the lowest singlet scalar becomes relevant below N_f^* which generates an RG flow dissolving the IR fixed points. A critical prediction of this mechanism is the singlet scalar approaching marginality condition $\Delta_{\text{Sig}} = 3$ from above near N_f^*, which is surprisingly consistent with the behavior of kinks in figure 1.

4 Discussions

In this work we have bootstrapped the SO(5) symmetric DQCP and our results suggest the phase transitions observed in previous lattice simulations cannot be both SO(5) symmetric and continuous. Moreover, we discovered a new family of kinks in the SO(N) vector bootstrap bounds with $N \geqslant 6$, while the SO(5) DQCP is just slightly below the window. These kinks show interesting fine structures which require more bootstrap data for a clear understanding. We observed bound coincidences between the SU(N_f) adjoint and SO(N_f^2-1) vector bootstrap and explained that this is caused by an algebraic relation between the two crossing equations. We have shown that for general large N_fs, with gaps breaking SO(N_f^2-1) symmetry the SU(N_f) adjoint bootstrap bounds converge to conformal QED$_3$. Our results support the merger and annihilation mechanism for the loss of conformality in QED$_3$, and indicate a critical flavor number of QED$_3$: $N_f^* \in (2, 4)$.

Our results are illuminating for the widely interested project on solving conformal QED$_3$ with bootstrap. On the one hand, our results indicate the CFT landscape is not tameless–after introducing suitable SO(N) symmetry breaking gaps the bootstrap bounds indeed get close to the conformal QED$_3$. On the other hand, our results also clarified that to numerically solve conformal QED$_3$ with bootstrap, a crucial challenge is to resolve the SO(N) symmetry enhancement in the crossing equations and reproduce proper spectrum of QED$_3$, for which certain substantially new ingredients are needed in conformal bootstrap.

Acknowledgments

The author thanks Miguel Costa, Zohar Komargodski, David Poland, Junchen Rong, Slava Rychkov, Christopher Pope, Ning Su and Cenke Xu for valuable discussions. The author is especially grateful to Christopher Pope for his consistent support throughout the course of this work. The author is greatly benefited from collaborations with Ning Su on numerical conformal bootstrap. The author would like to thank the organizers of the "Project Meeting: Analytical Approaches workshop at Azores and the Bootstrap 2018 workshop at Caltech, for their hospitality and support. This research received funding from the grant CERN/FIS-PAR/0019/2017. This work was also supported by the Southeast University and the Simons Foundation grant 488637 and 488651 (Simons collaboration on the Nonperturbative bootstrap) and the DOE grant no. DE-SC0020318. Centro de Física do Porto is partially funded by the Foundation for Science and Technology of Portugal (FCT). The computations in this work were run on the Mac Lab cluster supported by the Department of Physics and Astronomy, Texas A&M University, and the Yale Grace computing cluster, supported by the facilities and staff of the Yale University Faculty of Sciences High Performance Computing Center.

JHEP11(2022)005

A Relation between the SU(N_f) adjoint and SO(N_f^2-1) vector bootstrap

In this section we show more details on the algebraic relation between crossing equations of the SU(N_f) adjoint and SO(N_f^2-1) vector scalars. We will follow the methods developed in [57, 58] which were motivated by the new family of kinks discovered in this work. Combined with the bootstrap algorithm, this algebraic structure can explain the SO(N_f^2-1) symmetry enhancement in the SU(N_f) adjoint bootstrap bounds. It is also crucial in decoding the underlying theories of the new family of kinks, which were conjectured to be conformal QED$_3$ in this work.

Let us consider the four-point correlator of an SU(N_f) ($N_f \geqslant 4$) adjoint scalar $\mathcal{O}_{\rm ad}$

$$\langle \mathcal{O}_{\rm ad}(x_1)\mathcal{O}_{\rm ad}(x_2)\mathcal{O}_{\rm ad}(x_3)\mathcal{O}_{\rm ad}(x_4)\rangle. \tag{A.1}$$

There are six representations appearing in its conformal partial wave expansions, corresponding to the OPE

$$\mathcal{O}_{\rm ad}\times\mathcal{O}_{\rm ad} \to \mathbf{1}^+ \oplus \mathrm{Ad}^+ \oplus \mathrm{Ad}^- \oplus A\bar{A}^+ \oplus \left(T\bar{A}+A\bar{T}\right)^- \oplus T\bar{T}^+, \tag{A.2}$$

where the $\mathbf{1}$ and Ad denote the singlet and adjoint representations of SU(N_f). A/T ($\bar{A}/\bar{T}$) denote representations with anti-symmetric/symmetric fundamental (anti-fundamental) indices of SU(N_f). Moreover, operator $\mathcal{O}_{\rm ad}$ is real, so are the operators in its OPE, therefore only the real combination of representation $T\bar{A}$ and its complex conjugation $A\bar{T}$ can appear in (A.2). We use $T\bar{A}$ to denote this sector for simplicity. The superscripts in $R^\pm$ denote even/odd spin selection rules in the representation R.

Crossing equations of the four-point correlator (A.1) have been obtained in previous bootstrap studies [59, 60], which can be written in a compact form

$$\sum_{\mathcal{O}\in\ell^+}\lambda_{\mathcal{O}}^2\vec{V}_{\mathbf{1}}^+ + \sum_{\mathcal{O}\in\ell^+}\lambda_{\mathcal{O}}^2\vec{V}_{\rm Ad}^+ + \sum_{\mathcal{O}\in\ell^-}\lambda_{\mathcal{O}}^2\vec{V}_{\rm Ad}^- + \sum_{\mathcal{O}\in\ell^-}\lambda_{\mathcal{O}}^2\vec{V}_{T\bar{A}}^- + \sum_{\mathcal{O}\in\ell^+}\lambda_{\mathcal{O}}^2\vec{V}_{A\bar{A}}^+ + \sum_{\mathcal{O}\in\ell^+}\lambda_{\mathcal{O}}^2\vec{V}_{T\bar{T}}^+ = 0\,. \tag{A.3}$$

Here the vector $\vec{V}_R^\pm$ corresponds to the SU(N_f) representation R with even/odd spins. Explicit form of each vector can be summarized in the matrix $\mathcal{M}_{\rm ad}$ (3.1), which can be converted into the SO(N_f^2-1) vector crossing equations $\mathcal{M}_{SO(N_f^2-1)}$ (3.2) through the transformation $\mathscr{T}_{\rm ad}$ (3.3). Specifically, the action $\mathscr{T}_{\rm ad}\cdot\mathcal{M}_{\rm ad}$ (3.4) are given by

$$\begin{aligned}\mathscr{T}_{\rm ad}\cdot\mathcal{M}_{\rm ad} &= \begin{pmatrix} 0 & x_1 F & -x_2F & -x_3F & x_4F & x_5F \\ F & x_1F\left(1-\frac{2}{N_f^2-1}F\right) & x_2F & x_3F & x_4F\left(1-\frac{2}{N_f^2-1}\right)F & x_5F\left(1-\frac{2}{N_f^2-1}\right) \\ H & -x_1H\left(1+\frac{2}{N_f^2-1}\right)H & -x_2H & -x_3H & -x_4\left(1+\frac{2}{N_f^2-1}\right)H & -x_5\left(1+\frac{2}{N_f^2-1}\right)H \end{pmatrix} \\ &= \left(\vec{V}_{\rm Sig}^+,\, x_1\vec{V}_T^+,\, x_2\vec{V}_A^-,\, x_3\vec{V}_A^-,\, x_4\vec{V}_T^+,\, x_5\vec{V}_T^+\right),\end{aligned} \tag{A.4}$$

with positive coefficients $\vec{x}$

$$\vec{x} = \left\{\frac{2\left(N_f^4-5N_f^2+4\right)}{N_f\left(N_f^4-N_f^2-2\right)},\, \frac{2N_f}{N_f^2-2},\, 1-\frac{2}{N_f^2-2},\, \frac{(N_f-3)\,N_f^2\,(N_f+1)}{\left(N_f^2-2\right)\left(N_f^2+1\right)},\, \frac{(N_f-1)\,N_f^2\,(N_f+3)}{\left(N_f^2-2\right)\left(N_f^2+1\right)}\right\}. \tag{A.5}$$

JHEP11(2022)005

The right part of (A.4) is just the $\mathrm{SO}(N_f^2-1)$ vector crossing equations $\mathcal{M}_{SO(N_f^2-1)}$ associated with the $\mathrm{SO}(N_f^2-1) \to \mathrm{SU}(N_f)$ branching rules given by (3.5)–(3.7). The algebraic relation (A.4) connects the $\mathrm{SU}(N_f)$ adjoint bootstrap problem with the $\mathrm{SO}(N_f^2-1)$ vector bootstrap problem in the following way.

Assume we have obtained linear functionals $\vec{\alpha} \equiv (\alpha_1, \alpha_2, \alpha_3)$ for the $\mathrm{SO}(N_f^2-1)$ vector bootstrap, i.e.,

$$\vec{\alpha} \cdot \mathcal{M}_{SO(N_f^2-1)} = \vec{\alpha} \cdot \left(\vec{V}^+_{\mathrm{Sig}}, \vec{V}^+_T, \vec{V}^-_A\right) = \left(\alpha^+_{\mathrm{Sig}}, \alpha^+_T, \alpha^-_A\right) \succeq 0_{1\times 3}\,, \qquad \forall \Delta \geqslant \Delta^*_{\mathrm{Sig}/T/A,\ell}\,, \tag{A.6}$$

then the linear functionals $\vec{\alpha}$ could be used to construct linear functionals for the $\mathrm{SU}(N_f)$ adjoint bootstrap. Specifically, the action of the linear functionals $\vec{\beta} = \vec{\alpha} \cdot (\mathscr{T}_{\mathrm{ad}})$ on the $\mathrm{SU}(N_f)$ adjoint bootstrap equations is

$$\vec{\beta} \cdot \mathcal{M}_{\mathrm{ad}} = (\vec{\alpha} \cdot \mathscr{T}_{\mathrm{ad}}) \cdot \mathcal{M}_{\mathrm{ad}} = \vec{\alpha} \cdot \left(\vec{V}^+_{\mathrm{Sig}},\, x_1\vec{V}^+_T,\, x_2\vec{V}^-_A,\, x_3\vec{V}^-_A,\, x_4\vec{V}^+_T,\, x_5\vec{V}^+_T\right) \tag{A.7}$$

$$= \left(\alpha^+_{\mathrm{Sig}},\, x_1\alpha^+_T,\, x_2\alpha^-_A,\, x_3\alpha^-_A,\, x_4\alpha^+_T,\, x_5\alpha^+_T\right), \qquad \forall \Delta \geqslant \Delta^*_{R_i,\ell}\,. \tag{A.8}$$

As long as the gap assumptions $\Delta^*_{R_i,\ell}$ in (A.8) is consistent with the gap assumptions in (A.6), the linear functional actions in (A.8) also satisfy the positive conditions. This leads to a conclusion that any linear functionals that can be used to exclude the CFT data in $\mathrm{SO}(N_f^2-1)$ vector bootstrap can also be used to exclude the CFT data in $\mathrm{SU}(N_f)$ adjoint bootstrap. Also any $\mathrm{SO}(N_f^2-1)$ symmetric solutions to the crossing equations can be decomposed into the solutions of the $\mathrm{SU}(N_f)$ adjoint crossing equations. Therefore the bootstrap allowed regions of the two different bootstrap setup are actually exactly the same! The bootstrap bound coincidence was firstly observed between the singlet bounds in the $\mathrm{SU}(N)$ fundamental and $\mathrm{SO}(2N)$ vector bootstrap [67]. The $\mathrm{SU}(N_f)$ adjoint and $\mathrm{SO}(N_f^2-1)$ vector bootstrap bound coincidence studied in this work has also been noticed in [68]. If one adopts different gap assumptions explicitly breaking the $\mathrm{SO}(N_f^2-1) \to \mathrm{SU}(N_f)$ branching rules (3.5)–(3.7), then bootstrap results from the two different implementations will show differences.

In summary, the $\mathrm{SU}(N_f)$ adjoint crossing equations have the same positivity structure as the $\mathrm{SO}(N_f^2-1)$ vector crossing equations. To bootstrap the non-$\mathrm{SO}(N)$ symmetric theories like conformal QED_3, it is necessary to introduce gaps in the bootstrap equations which break the $\mathrm{SO}(N_f^2-1)$ symmetry explicitly. In this work, we introduce gap assumptions consistent with QED_3 spectrum and compare the bootstrap bounds with $1/N_f$ perturbative results of conformal QED_3.

For the linear extrapolations in table 2, we have computed Δ_4 upper bounds to the numerical precision 10^{-5} with $\Delta_{\mathcal{O}_{\mathrm{ad}}}$ fixed at the large N_f perturbative result [69]

$$\Delta_{\mathcal{O}_{\mathrm{ad}}} = 2 - \frac{64}{3\pi^2 N_f} + \frac{256\,(28 - 3\pi^2)}{9\pi^4 N_f^2}\,. \tag{A.9}$$

The data is provided in an attached *Mathematica* file.

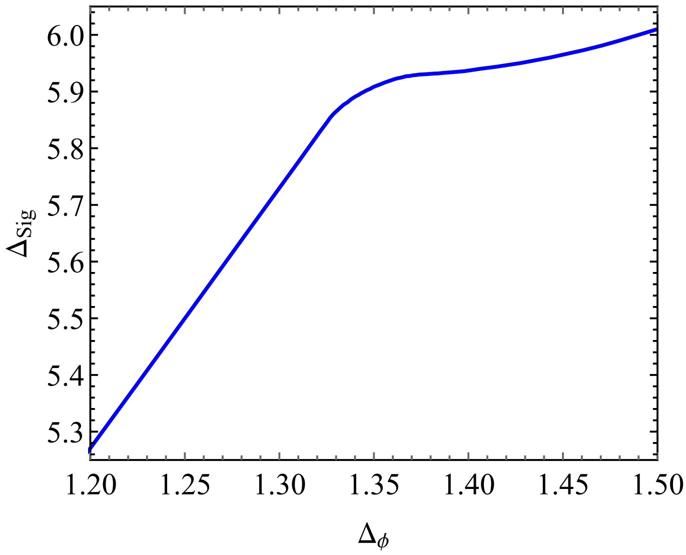

Figure 6. Bound ($\Lambda = 31$) on the scaling dimension of the lowest $\mathrm{SO}(4^2 - 1)$ singlet scalar.

B Two adjacent kinks in the SO(N) singlet bound?

In this section we study fine structures of the new family of kinks in the bounds on SO(N) singlet scalars. As shown in the zoomed in subplot in figure 4, the new family of kinks in the SO(N) singlet bounds may have fine structures with two nearby kinks for large Ns. Such fine structure is not shown or indistinguishable in the singlet bounds with small Ns, see e.g. figure 1. In the $\mathrm{SO}(20^2 - 1)$ singlet bound shown in figure 4, there is a prominent first kink near $\Delta_\phi \sim 1.9$, followed by another mild kink near $\Delta_\phi \in (1.94, 1.95)$. Comparing with the jump in the bound on the scaling dimension of the lowest $O(20^2 - 1)$ traceless symmetric scalar Δ_T, we notice that the second kink in the singlet bound has scaling dimension Δ_ϕ close to the top of the jump, while Δ_ϕ of the first kink, which is close to $N_f = 20$ QED_3 relates to the bottom of the jump.

In figure 6 we provide another example for the kink in the SO(15) singlet bound. The SO(15) vector bootstrap bounds on the singlet and traceless symmetric scalars have been shown in figure 3 (purple lines). Figure 6 shows the zoomed in singlet bound near the kink. Comparing with kinks with small Ns in figure 1, the kink(s) in figure 6 spread in a notable region with two transitions. In the bound on Δ_T, $N = 15$ is not large enough to form a sharp jump, while the range of Δ_ϕ of the singlet kink(s) in figure 6 is close to the kink in the bound on Δ_T.

C More discussions on the gap Δ_1^* in the spin 1 $T\bar{A}$ sector

In figure 4 we have shown that with gaps $\Delta_1^* = 4.5, 4.8,$ or 5.0 on the spin 1 operators in $T\bar{A}$ sector, bootstrap bounds on Δ_4 can form sharp jumps whose positions depend on the specific values of Δ_1^*. In this section we provide more discussions on the bootstrap results. We reproduce bootstrap bounds on Δ_4 in figure 7 for convenience.

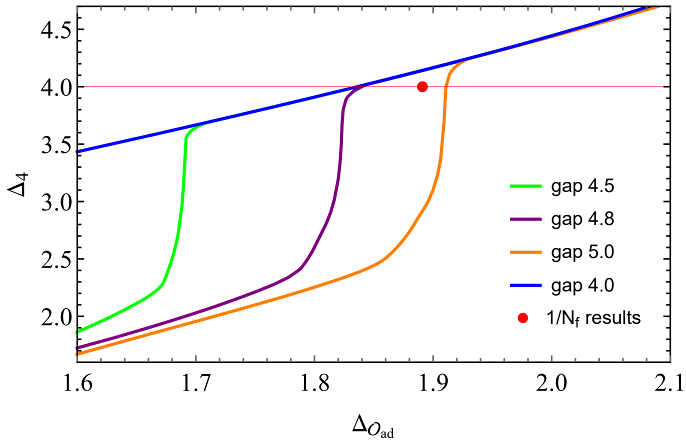

Figure 7. Bounds on Δ_4 with different gap assumptions Δ_1^* on the lowest spin 1 operator in the $T\bar{A}$ sector.

The lowest spin 1 operator in $T\bar{A}$ sector has scaling dimension $5\pm 1/N_f$. The subleading order correction is not known yet. The physical gap Δ_1^* could be slightly above or below 5 for $N_f=20$, depending on the sign of the subleading order correction. An interesting observation in figure 7 is that with a gap $\Delta_1^*=5$, the large N_f predictions on QED$_3$ $(\Delta_{\mathcal{O}_{\rm ad}},\Delta_4)\simeq(1.891,4.0)$ are excluded! Note $\Delta_{\mathcal{O}_{\rm ad}}\simeq 1.891$ is given by $1/N_f$ perturbative result at the order $1/N_f^2$, which is expected to be well close to the physical spectrum. $\Delta_4\simeq 4$ is given by large N_f expansions on the scaling dimensions of the four-fermion operators (3.8), which can be shifted by higher order corrections while it is unlikely to be lowered into the bootstrap allowed region in figure 7: $\Delta_4<3$ at $\Delta_{\mathcal{O}_{\rm ad}}=1.891$. We expect the $1/N_f$ predictions on QED$_3$ are excluded due to the gap assumption $\Delta_1^*=5$. The physical gap Δ_1^* should be smaller than 5 and the subleading order correction is negative.

Moreover, with a gap $\Delta_1^*=4.8$ the top of the jump is close to the physical value $\Delta_4=4$. Near the jump we have $\Delta_{\mathcal{O}_{\rm ad}}\simeq 1.84$, smaller than the large N_f prediction $\Delta_{\mathcal{O}_{\rm ad}}\simeq 1.89$. As shown in the linear extrapolation of bound on Δ_4, the large Λ extrapolation will help to reduce the discrepancy. It is interesting to compare with subleading order corrections on the four-fermion scalars (3.8). For $N_f=20$ QED$_3$ the formulas in (3.8) give anomalous dimensions $\Delta_R^{(1)}$:

$$\left(\Delta^{(1)}_{\rm Ad},\Delta^{(1)}_{A\bar{A}},\Delta^{(1)}_{T\bar{T}}\right)\simeq(-0.31,-0.32,0.11), \tag{C.1}$$

close to the "anomalous dimension" -0.2 given by the gap $\Delta_1^*=4.8$. A critical question is when the gap Δ_1^* is close to the physical spectrum of the lowest spin 1 operator in $T\bar{A}$, will the top of the jump in the bound on Δ_4 get close to QED$_3$? It is also interesting to isolate QED$_3$ solutions near the jumps using single correlator bootstrap [70]. We will provide a more comprehensive study for this problem in the near future.

It is quite encouraging that with a suitable gap in $T\bar{A}$ sector, bootstrap bound can form a sharp jump close to the physical spectrum. On the other hand, our results disclose a subtle challenge to solve conformal QED$_3$ using conformal bootstrap. The bootstrap bounds, in particular the kinks depend on gaps imposed in the bootstrap equations. Therefore one has to resort to the results from large N_f expansions or other approaches to obtain bootstrap bounds relevant to QED_3. Reliable information on QED_3 is not available for physically interested theories with small N_f and our hope is to solve QED_3 without specific information of the theory. It is important to find new ingredients to resolve the gap-dependence problem for future bootstrap studies.

References

[1] A.M. Polyakov, *Compact Gauge Fields and the Infrared Catastrophe*, Phys. Lett. B **59** (1975) 82 [INSPIRE].

[2] A.M. Polyakov, *Quark Confinement and Topology of Gauge Groups*, Nucl. Phys. B **120** (1977) 429 [INSPIRE].

[3] T. Appelquist, D. Nash and L.C.R. Wijewardhana, *Critical Behavior in* $(2+1)$*-Dimensional QED*, Phys. Rev. Lett. **60** (1988) 2575 [INSPIRE].

[4] R.D. Pisarski, *Chiral Symmetry Breaking in Three-Dimensional Electrodynamics*, Phys. Rev. D **29** (1984) 2423 [INSPIRE].

[5] T.W. Appelquist, M.J. Bowick, D. Karabali and L.C.R. Wijewardhana, *Spontaneous Chiral Symmetry Breaking in Three-Dimensional QED*, Phys. Rev. D **33** (1986) 3704 [INSPIRE].

[6] W. Rantner and X.-G. Wen, *Electron spectral function and algebraic spin liquid for the normal state of underdoped high* T_c *superconductors*, Phys. Rev. Lett. **86** (2001) 3871 [cond-mat/0010378] [INSPIRE].

[7] W. Rantner and X.-G. Wen, *Spin correlations in the algebraic spin liquid: Implications for high-Tc superconductors*, Phys. Rev. B **66** (2002) 144501 [cond-mat/0201521] [INSPIRE].

[8] K.-i. Kubota and H. Terao, *Dynamical symmetry breaking in* QED_3 *from the Wilson RG point of view*, Prog. Theor. Phys. **105** (2001) 809 [hep-ph/0101073] [INSPIRE].

[9] A.V. Kotikov, V.I. Shilin and S. Teber, *Critical behavior of* $(2+1)$*-dimensional QED: 1/*N_f *corrections in the Landau gauge*, Phys. Rev. D **94** (2016) 056009 [*Erratum ibid.* **99** (2019) 119901] [arXiv:1605.01911] [INSPIRE].

[10] K. Kaveh and I.F. Herbut, *Chiral symmetry breaking in* QED_3 *in presence of irrelevant interactions: A Renormalization group study*, Phys. Rev. B **71** (2005) 184519 [cond-mat/0411594] [INSPIRE].

[11] S. Giombi, I.R. Klebanov and G. Tarnopolsky, *Conformal* QED_d*, F-Theorem and the* ϵ *Expansion*, J. Phys. A **49** (2016) 135403 [arXiv:1508.06354] [INSPIRE].

[12] L. Di Pietro, Z. Komargodski, I. Shamir and E. Stamou, *Quantum Electrodynamics in* $d=3$ *from the* ε *Expansion*, Phys. Rev. Lett. **116** (2016) 131601 [arXiv:1508.06278] [INSPIRE].

[13] S. Giombi, G. Tarnopolsky and I.R. Klebanov, *On* C_J *and* C_T *in Conformal QED*, JHEP **08** (2016) 156 [arXiv:1602.01076] [INSPIRE].

[14] N. Zerf, P. Marquard, R. Boyack and J. Maciejko, *Critical behavior of the QED_3-Gross-Neveu-Yukawa model at four loops*, *Phys. Rev. B* **98** (2018) 165125 [arXiv:1808.00549] [INSPIRE].

[15] I.F. Herbut, *Chiral symmetry breaking in three-dimensional quantum electrodynamics as fixed point annihilation*, *Phys. Rev. D* **94** (2016) 025036 [arXiv:1605.09482] [INSPIRE].

[16] V.P. Gusynin and P.K. Pyatkovskiy, *Critical number of fermions in three-dimensional QED*, *Phys. Rev. D* **94** (2016) 125009 [arXiv:1607.08582] [INSPIRE].

[17] S. Benvenuti and H. Khachatryan, *Qed's in* 2+1 *dimensions: complex fixed points and dualities*, arXiv:1812.01544.

[18] J. Braun, H. Gies, L. Janssen and D. Roscher, *Phase structure of many-flavor QED_3*, *Phys. Rev. D* **90** (2014) 036002 [arXiv:1404.1362] [INSPIRE].

[19] S. Gukov, *RG Flows and Bifurcations*, *Nucl. Phys. B* **919** (2017) 583 [arXiv:1608.06638] [INSPIRE].

[20] S.J. Hands, J.B. Kogut, L. Scorzato and C.G. Strouthos, *The Chiral limit of noncompact QED in three-dimensions*, *Nucl. Phys. B Proc. Suppl.* **119** (2003) 974 [hep-lat/0209133] [INSPIRE].

[21] S.J. Hands, J.B. Kogut and C.G. Strouthos, *Noncompact QED_3 with N_f greater than or equal to* 2, *Nucl. Phys. B* **645** (2002) 321 [hep-lat/0208030] [INSPIRE].

[22] S.J. Hands, J.B. Kogut, L. Scorzato and C.G. Strouthos, *Non-compact QED_3 with $N_f = 1$ and $N_f = 4$*, *Phys. Rev. B* **70** (2004) 104501 [hep-lat/0404013] [INSPIRE].

[23] C. Strouthos and J.B. Kogut, *The Phases of Non-Compact QED_3*, *PoS* **LATTICE2007** (2007) 278 [arXiv:0804.0300] [INSPIRE].

[24] N. Karthik and R. Narayanan, *No evidence for bilinear condensate in parity-invariant three-dimensional QED with massless fermions*, *Phys. Rev. D* **93** (2016) 045020 [arXiv:1512.02993] [INSPIRE].

[25] N. Karthik and R. Narayanan, *Scale-invariance of parity-invariant three-dimensional QED*, *Phys. Rev. D* **94** (2016) 065026 [arXiv:1606.04109] [INSPIRE].

[26] T. Senthil, A. Vishwanath, L. Balents, S. Sachdev and M.P.A. Fisher, *Deconfined Quantum Critical Points*, *Science* **303** (2004) 1490 [cond-mat/0311326] [INSPIRE].

[27] A. Karch and D. Tong, *Particle-Vortex Duality from 3d Bosonization*, *Phys. Rev. X* **6** (2016) 031043 [arXiv:1606.01893] [INSPIRE].

[28] N. Seiberg, T. Senthil, C. Wang and E. Witten, *A Duality Web in* $2+1$ *Dimensions and Condensed Matter Physics*, *Annals Phys.* **374** (2016) 395 [arXiv:1606.01989] [INSPIRE].

[29] C. Wang, A. Nahum, M.A. Metlitski, C. Xu and T. Senthil, *Deconfined quantum critical points: symmetries and dualities*, *Phys. Rev. X* **7** (2017) 031051 [arXiv:1703.02426] [INSPIRE].

[30] T. Senthil, D.T. Son, C. Wang and C. Xu, *Duality between* $(2+1)d$ *Quantum Critical Points*, *Phys. Rept.* **827** (2019) 1 [arXiv:1810.05174] [INSPIRE].

[31] A. Nahum, J.T. Chalker, P. Serna, M. Ortuño and A.M. Somoza, *Deconfined Quantum Criticality, Scaling Violations, and Classical Loop Models*, *Phys. Rev. X* **5** (2015) 041048 [arXiv:1506.06798] [INSPIRE].

[32] A. Nahum, P. Serna, J.T. Chalker, M. Ortuño and A.M. Somoza, *Emergent* SO(5) *Symmetry at the Néel to Valence-Bond-Solid Transition*, *Phys. Rev. Lett.* **115** (2015) 267203 [arXiv:1508.06668] [INSPIRE].

JHEP11(2022)005

[33] Y.Q. Qin et al., *Duality between the deconfined quantum-critical point and the bosonic topological transition*, Phys. Rev. X **7** (2017) 031052 [arXiv:1705.10670] [INSPIRE].

[34] G.J. Sreejith, S. Powell and A. Nahum, *Emergent* SO(5) *symmetry at the columnar ordering transition in the classical cubic dimer model*, Phys. Rev. Lett. **122** (2019) 080601 [arXiv:1803.11218] [INSPIRE].

[35] P. Serna and A. Nahum, *Emergence and spontaneous breaking of approximate $O(4)$ symmetry at a weakly first-order deconfined phase transition*, Phys. Rev. B **99** (2019) 195110 [arXiv:1805.03759] [INSPIRE].

[36] X.Y. Xu, Y. Qi, L. Zhang, F.F. Assaad, C. Xu and Z.Y. Meng, *Monte Carlo Study of Lattice Compact Quantum Electrodynamics with Fermionic Matter: The Parent State of Quantum Phases*, Phys. Rev. X **9** (2019) 021022 [arXiv:1807.07574] [INSPIRE].

[37] R. Rattazzi, V.S. Rychkov, E. Tonni and A. Vichi, *Bounding scalar operator dimensions in 4D CFT*, JHEP **12** (2008) 031 [arXiv:0807.0004] [INSPIRE].

[38] D. Poland, S. Rychkov and A. Vichi, *The Conformal Bootstrap: Theory, Numerical Techniques, and Applications*, Rev. Mod. Phys. **91** (2019) 015002 [arXiv:1805.04405] [INSPIRE].

[39] S.M. Chester and S.S. Pufu, *Towards bootstrapping QED_3*, JHEP **08** (2016) 019 [arXiv:1601.03476] [INSPIRE].

[40] S.M. Chester, L.V. Iliesiu, M. Mezei and S.S. Pufu, *Monopole Operators in* U(1) *Chern-Simons-Matter Theories*, JHEP **05** (2018) 157 [arXiv:1710.00654] [INSPIRE].

[41] Y. Nakayama and T. Ohtsuki, *Conformal Bootstrap Dashing Hopes of Emergent Symmetry*, Phys. Rev. Lett. **117** (2016) 131601 [arXiv:1602.07295] [INSPIRE].

[42] Y. Nakayama, unpublished.

[43] D. Simmons-Duffin, unpublished.

[44] D. Poland, unpublished.

[45] A.W. Sandvik, *Evidence for deconfined quantum criticality in a two-dimensional Heisenberg model with four-spin interactions*, Phys. Rev. Lett. **98** (2007) 227202 [cond-mat/0611343] [INSPIRE].

[46] R.G. Melko and R.K. Kaul, *Scaling in the fan of an unconventional quantum critical point*, Phys. Rev. Lett. **100** (2008).

[47] S. Pujari, K. Damle and F. Alet, *Néel-state to valence-bond-solid transition on the honeycomb lattice: Evidence for deconfined criticality*, Phys. Rev. Lett. **111** (2013).

[48] E. Dyer, M. Mezei, S.S. Pufu and S. Sachdev, *Scaling dimensions of monopole operators in the $\mathbb{CP}^{N_b-1}$ theory in $2+1$ dimensions*, JHEP **06** (2015) 037 [*Erratum ibid.* **03** (2016) 111] [arXiv:1504.00368] [INSPIRE].

[49] E. Dupuis, R. Boyack and W. Witczak-Krempa, *Anomalous Dimensions of Monopole Operators at the Transitions between Dirac and Topological Spin Liquids*, Phys. Rev. X **12** (2022) 031012 [arXiv:2108.05922] [INSPIRE].

[50] R. Boyack, A. Rayyan and J. Maciejko, *Deconfined criticality in the QED3 Gross-Neveu-Yukawa model: The $1/N$ expansion revisited*, Phys. Rev. B **99** (2019) 195135 [arXiv:1812.02720] [INSPIRE].

[51] D. Simmons-Duffin, *A Semidefinite Program Solver for the Conformal Bootstrap*, JHEP **06** (2015) 174 [arXiv:1502.02033] [INSPIRE].

JHEP11(2022)005

[52] F. Kos, D. Poland and D. Simmons-Duffin, *Bootstrapping the $O(N)$ vector models*, *JHEP* **06** (2014) 091 [arXiv:1307.6856] [INSPIRE].

[53] H. Gies and J. Jaeckel, *Chiral phase structure of QCD with many flavors*, *Eur. Phys. J. C* **46** (2006) 433 [hep-ph/0507171] [INSPIRE].

[54] D.B. Kaplan, J.-W. Lee, D.T. Son and M.A. Stephanov, *Conformality Lost*, *Phys. Rev. D* **80** (2009) 125005 [arXiv:0905.4752] [INSPIRE].

[55] V. Gorbenko, S. Rychkov and B. Zan, *Walking, Weak first-order transitions, and Complex CFTs*, *JHEP* **10** (2018) 108 [arXiv:1807.11512] [INSPIRE].

[56] J.A. Gracey, *Fermion bilinear operator critical exponents at $O(1/N^2)$ in the QED-Gross-Neveu universality class*, *Phys. Rev. D* **98** (2018) 085012 [arXiv:1808.07697] [INSPIRE].

[57] Z. Li and D. Poland, *Searching for gauge theories with the conformal bootstrap*, *JHEP* **03** (2021) 172 [arXiv:2005.01721] [INSPIRE].

[58] Z. Li, *Symmetries of conformal correlation functions*, *Phys. Rev. D* **105** (2022) 085018 [arXiv:2006.05119] [INSPIRE].

[59] M. Berkooz, R. Yacoby and A. Zait, *Bounds on $\mathcal{N}=1$ superconformal theories with global symmetries*, *JHEP* **08** (2014) 008 [*Erratum ibid.* **01** (2015) 132] [arXiv:1402.6068] [INSPIRE].

[60] H. Iha, H. Makino and H. Suzuki, *Upper bound on the mass anomalous dimension in many-flavor gauge theories: a conformal bootstrap approach*, *PTEP* **2016** (2016) 053B03 [arXiv:1603.01995] [INSPIRE].

[61] F.A. Dolan and H. Osborn, *Conformal four point functions and the operator product expansion*, *Nucl. Phys. B* **599** (2001) 459 [hep-th/0011040] [INSPIRE].

[62] F.A. Dolan and H. Osborn, *Conformal partial waves and the operator product expansion*, *Nucl. Phys. B* **678** (2004) 491 [hep-th/0309180] [INSPIRE].

[63] C. Xu, *Renormalization group studies on four-fermion interaction instabilities on algebraic spin liquids*, *Phys. Rev. B* **78** (2008) 054432.

[64] S.M. Chester and S.S. Pufu, *Anomalous dimensions of scalar operators in QED_3*, *JHEP* **08** (2016) 069 [arXiv:1603.05582] [INSPIRE].

[65] J.Y. Lee, C. Wang, M.P. Zaletel, A. Vishwanath and Y.-C. He, *Emergent Multi-flavor QED_3 at the Plateau Transition between Fractional Chern Insulators: Applications to graphene heterostructures*, *Phys. Rev. X* **8** (2018) 031015 [arXiv:1802.09538] [INSPIRE].

[66] V. Gorbenko, S. Rychkov and B. Zan, *Walking, Weak first-order transitions, and Complex CFTs II. Two-dimensional Potts model at $Q>4$*, *SciPost Phys.* **5** (2018) 050 [arXiv:1808.04380] [INSPIRE].

[67] D. Poland, D. Simmons-Duffin and A. Vichi, *Carving Out the Space of 4D CFTs*, *JHEP* **05** (2012) 110 [arXiv:1109.5176] [INSPIRE].

[68] Y. Nakayama, *Bootstrap experiments on higher dimensional CFTs*, *Int. J. Mod. Phys. A* **33** (2018) 1850036 [arXiv:1705.02744] [INSPIRE].

[69] J.A. Gracey, *Electron mass anomalous dimension at $O(1/(N_f^2)$ in quantum electrodynamics*, *Phys. Lett. B* **317** (1993) 415 [hep-th/9309092] [INSPIRE].

[70] Z. Li and N. Su, *3D CFT Archipelago from Single Correlator Bootstrap*, *Phys. Lett. B* **797** (2019) 134920 [arXiv:1706.06960] [INSPIRE].

JHEP11(2022)005